

## Numerical determination of fatigue crack growth in 3D structures consisting of non-homogeneous and/or non-isotropic materials

Markus Fulland<sup>1, a</sup>, Martin Steigemann<sup>2, b</sup>, Hans A. Richard<sup>3, c</sup>  
and Maria Specovius-Neugebauer<sup>2, d</sup>

<sup>1</sup>Westfälisches Umwelt Zentrum, Universität Paderborn, Pohlweg 55, 33098 Paderborn, Germany

<sup>2</sup>Institute of Analysis and Applied Mathematics, University of Kassel, Heinrich-Plett-Str. 40,  
34132 Kassel, Germany

<sup>3</sup>Institute of Applied Mechanics, Universität Paderborn, Pohlweg 47-49, 33098 Paderborn,  
Germany

<sup>a</sup>fulland@fam.upb.de, <sup>b</sup>martin.steigemann@mathematik.uni-kassel.de, <sup>c</sup>richard@fam.upb.de,  
<sup>d</sup>specovi@mathematik.uni-kassel.de

**Keywords:** fatigue crack growth, numerical simulation, functionally graded materials, ADAPCRACK3D.

**Abstract.** Within the scope of this contribution the numerical simulation of crack propagation processes in three-dimensional structures under consideration of material inhomogeneities as well as effects of non-isotropy will be discussed. The inhomogeneity of a material thereby is realised not by a continuous, but by a discrete approach with a number of material interfaces. In the context of an automatic 3D-simulation the correct assignment of material properties to the new elements, which need to be generated in the process of mesh adaptation due to crack propagation is a special issue. For orthotropic materials the correct numerical calculation of stress intensity factors is bit more complicated. Those problems will extensively be discussed. Additional simulation examples will demonstrate the capability of the new program features.

### Introduction

In modern engineering an increasing amount of non-homogeneous and/or non-isotropic materials (e.g. laminates, composites, functionally graded materials) are employed in order to meet the more and more specialised demands on structural components with respect to structural integrity, wear resistance, damping facilities, crack growth resistance etc. For means of a reliable fracture mechanical assessment it is necessary to be able to automatically simulate crack propagation processes in three-dimensional structures consisting of such materials. For this purpose the 3D crack growth simulation program ADAPCRACK3D, which was developed at the Institute of Applied Mechanics at Universität Paderborn, is applied. Recent extensions of this program include orthotropic material behaviour as well as the possibility to create boundary layers within a structure by definition of different material properties. Those boundary layers do have major impact on the stress intensities at a crack front in their immediate vicinity. This interface approach incorporates some technical difficulties in the mesh adaptation with respect to crack growth which will be discussed in detail.

### 3D Crack growth simulation program ADAPCRACK3D

The numerical crack growth simulations are carried out with the program system ADAPCRACK3D [1]. Figure 1 shows its simplified functionality scheme. Basically the program

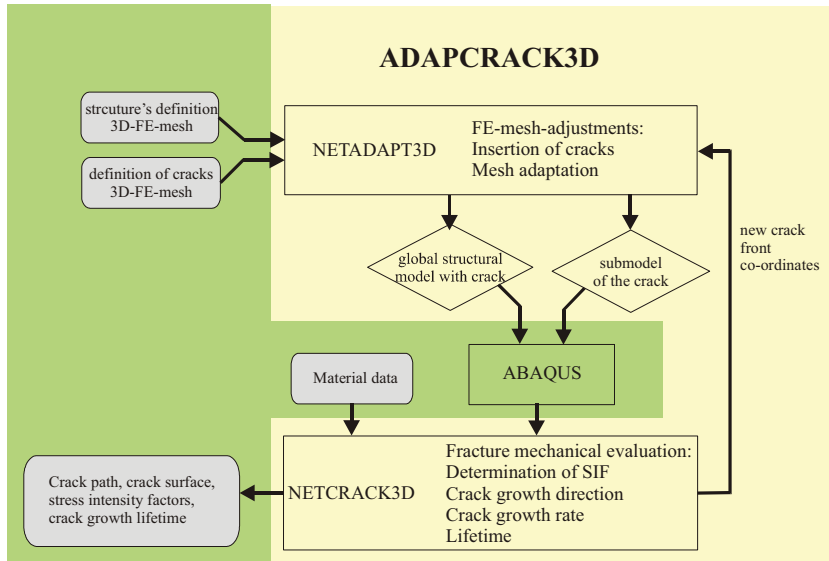


Figure 1: Functionality scheme of the program ADAPCRACK3D

consists of three modules NETADAPT3D, ABAQUS and NETCRACK3D. During the program run NETADAPT3D carries out the automatic adaptation of the finite element mesh to the geometry change, that is caused by the growing crack. The commercial finite element code ABAQUS is used as FE-solver. Thereby both the global model of the structure (including the crack) and a submodel of the immediate crack front vicinity are solved. The fracture mechanical evaluation is accomplished by the module NETCRACK3D on the basis of the submodel's solution. By use of the MVCCI-method [2],[3] at first energy release rates and subsequently stress intensity factors for all three fracture modes can be calculated. Afterwards the crack path and thus new crack front coordinates for the following simulation step can be determined. This is done by application of the  $\sigma_1$ -criterion[4]. This "standard workflow" needs to be adjusted in two critical points, if the material under consideration is no longer homogeneous and isotropic. For orthotropic materials the determination of stress intensity factors is different from the usual procedure, while in case, the structure does not consist of just one material, the mesh adaptation process for the global as well as for the sub-model has to be adjusted to this. Both issues will be discussed in the following.

### Mesh adaptation at material interfaces of the global model

Generally two different approaches are possible in order to realise crack growth through an interface within the program system ADAPCRACK3D automatically. The basic mesh adaptation is carried out by a modified Delaunay-algorithm, that is used for (FE-) node insertions into the existing mesh [5]. If the geometrical shape of the interface is to be strictly respected, this algorithm has to be adapted in a way, that forbids any element generation across the interface (Figure 2c,d). From an algorithmic point of view, this (additional) constraint is identical with the one prohibiting a break through the already existing crack surface during the local re-meshing procedure. However, it easily becomes evident, that the more constraints have to be fulfilled by the Delaunay-algorithm (crack and interface!) the more it loses its numerical stability. So a different approach is favoured, in which the interface during the geometrical crack adaptation in a first step is not taken into consideration. In a subsequent second step the material behaviour is assigned to the newly generated elements in an approximate manner. Consequently a "fuzziness" of the interface with a maximum width of an

element diameter is created (Figure 3). By appropriate mesh refinement the hereby induced error can be reduced to an acceptable magnitude.

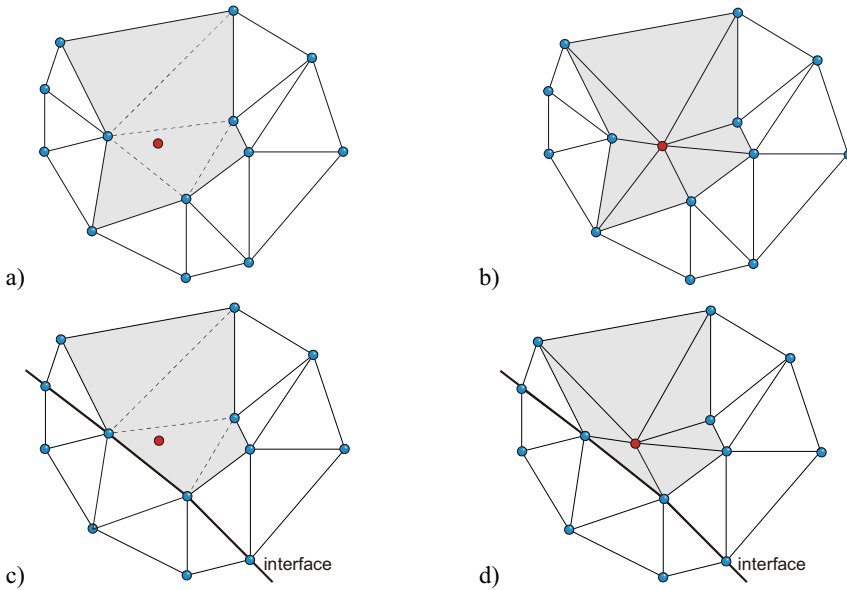


Figure 2: Insertion of an FE-node into the existing mesh using the Delaunay-algorithm a,b) within a homogeneous material c,d) in the vicinity of an interfaces while strictly respecting it

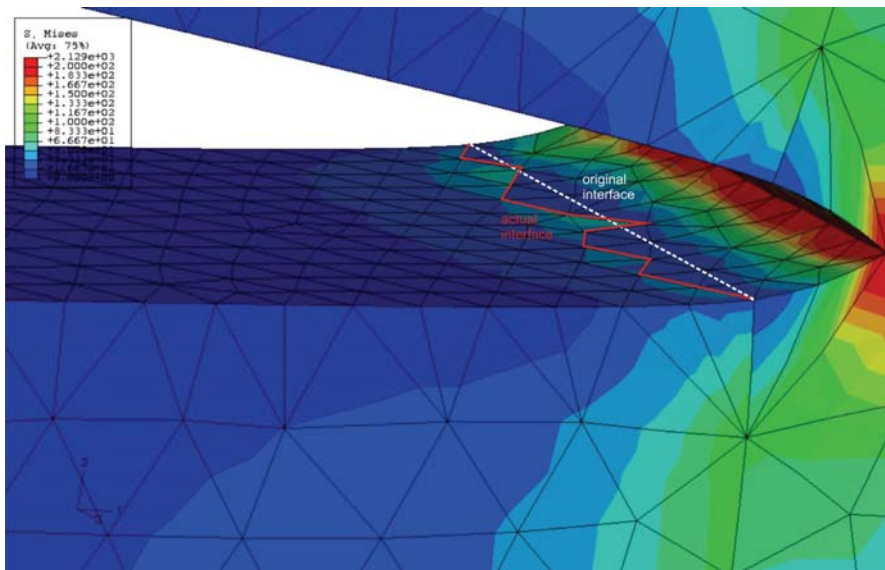


Figure 3: Local change of the interface due to automatic crack insertion process

**Numerical simulation of crack growth - inhomogeneous material**

The numerical simulations exemplifying the capabilities of the program with respect to inhomogeneous material behaviour are carried out by means of a standard CT-specimen (Figure 4). The (variable) position of the interface thereby is denoted with “g”, while the crack length is “a” in the given coordinate system. For the numerical investigations two different materials, an aluminium alloy ( $E=70656 \text{ N/mm}^2$ ,  $\nu=0.34$ ) and a steel ( $E=210000 \text{ N/mm}^2$ ,  $\nu=0.3$ ) are applied. The existence of the interface leads to general stress distributions as depicted in Figure 5.

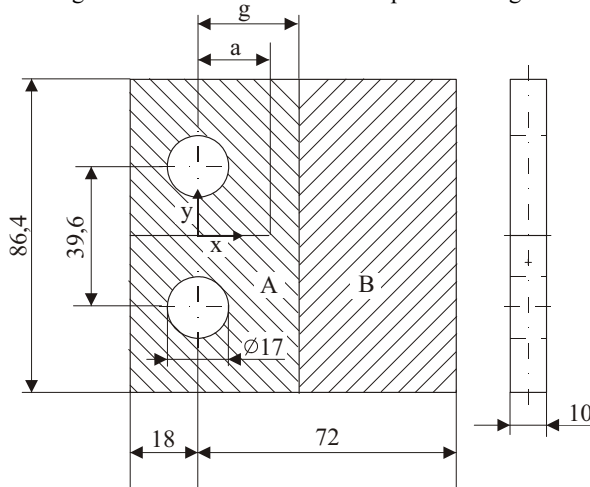


Figure 4: Dimensions of the investigated CT-specimen with interface between materials A and B

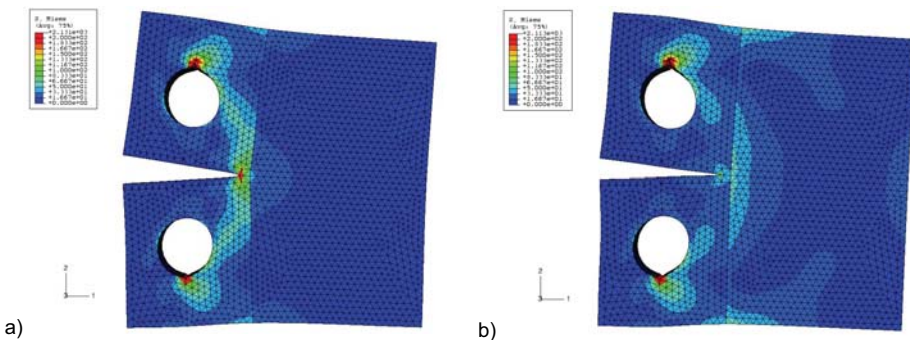


Figure 5: Stress distribution in dependence of the material arrangement, interface at  $g=20\text{mm}$ , crack length  $a=17\text{mm}$

- a) material A: steel, material B: aluminium alloy,
- b) material A: aluminum alloy, material B: steel

It is obvious, that the force flow is attuned in a way, that the stiffer steel bears a disproportionately high amount of the load. The fracture mechanical evaluation of the stress intensity factors yields the expected distribution. For a fixed crack length and concurrent variation of the interface position (Figure 6) it can be seen, that during transition from a weaker to a stiffer material (blue curve) the stress intensity decreases, while the crack front approaches the interface. After crossing the interface, the stress intensity re-increases up to the nominal value (left part of the curve). In the inverse case of a transition from a stiffer to a weaker material (magenta curve) the opposite effect is

observable. While approaching the interface, the stress intensity strongly increases. When comparing both curves, it becomes apparent, that the interface influences the stress intensity over a quite long distance, if it is in front of the crack tip: A notable difference to the nominal stress intensity factor for the homogeneous case can be found up to a interface position of  $g=68\text{mm}$ , (i.e.  $51\text{mm}$  in front of the crack front). On the other hand side, the influence quite fast vanishes after the crack has proceeded through the interface (left parts of the curves). From this it can be concluded, that the general development of the stress intensity factors are reproduced correctly by the program ADAPCRACK3D. The theoretical stress intensities  $K=0$  directly at the interface "aluminium $\rightarrow$ steel" and  $K=4$  at the interface "steel $\rightarrow$ aluminium" (comp. [6]), naturally cannot be captured exactly. However, by adjustment of the discretisation and the size of the submodel it is possible to approximate those values appropriately.

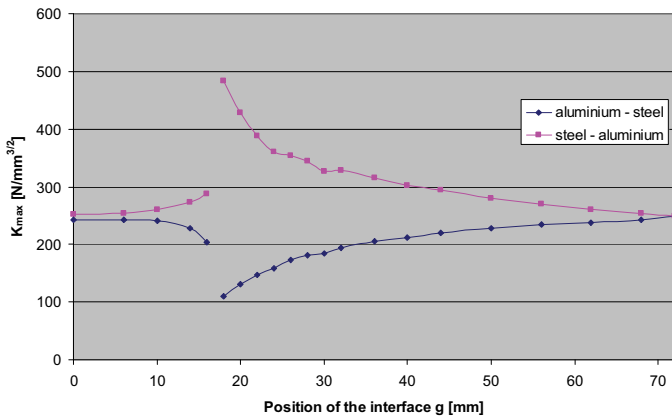


Figure 6: Development of the stress intensity factor for a fixed crack length  $a=17\text{mm}$  in dependence of the interface position

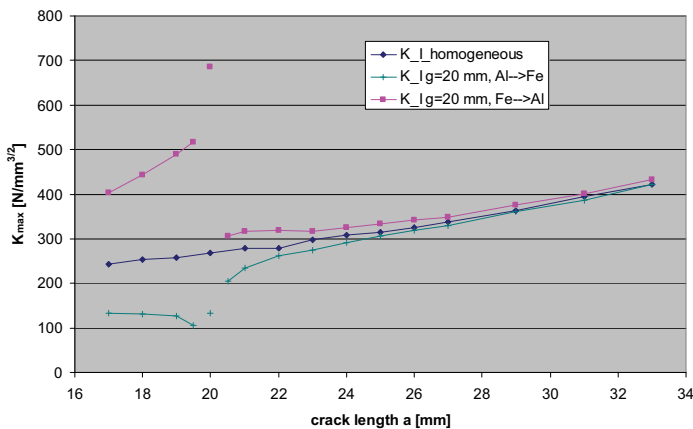


Figure 7: Development of the stress intensity for a fixed interface position  $g=20\text{mm}$  in dependence of the crack length

Figure 7 presents the development of the stress intensity with increasing crack length for a fixed interface position  $g=20\text{mm}$ . Also in this diagram it becomes apparent, that with approach of the crack front towards the interface at first a strong increase (transition steel  $\rightarrow$  aluminium, Figure 7a), or a strong decrease (transition aluminium  $\rightarrow$  steel, Figure 7b) can be observed. Almost immediately after the crack has crossed the interface, the stress intensities only marginally differ from the homogeneous solution.

**Numerical simulation of crack growth - orthotropic material**

The determination of stress intensity factors for orthotropic materials is a bit more complicated than in the standard isotropic case. In ADAPCRACK3D – as already mentioned – the well established MVCCI-method is applied in order to calculate the energy release rates for the different fracture modes. This is a straightforward procedure, since no assumptions concerning the elastic properties of the material are made in the method’s theory. However, the subsequent conversion into stress intensity factors is different from the isotropic case, because the stress intensity factors are no longer uncoupled [8]:

$$G_I = -\frac{K_I}{2} \frac{1}{E_2} \text{Im} \left[ \frac{K_I (\mu_1^{ip} + \mu_2^{ip}) + K_{II}}{\mu_1^{ip} \mu_2^{ip}} \right] \tag{1}$$

$$G_{II} = \frac{K_{II}}{2} \frac{1}{E_1} \text{Im} [K_{II} (\mu_1^{ip} + \mu_2^{ip}) + K_I \mu_1^{ip} \mu_2^{ip}]$$

where  $\mu_1$  and  $\mu_2$  are the roots of

$$\frac{1}{E_1} \mu^4 + \left( 2 \frac{-V_{12}}{E_1} + \frac{1}{G_{21}} \right) \mu^2 + \frac{1}{E_2} = 0. \tag{2}$$

Unfortunately so far no formulation also taking Mode III into account is available.

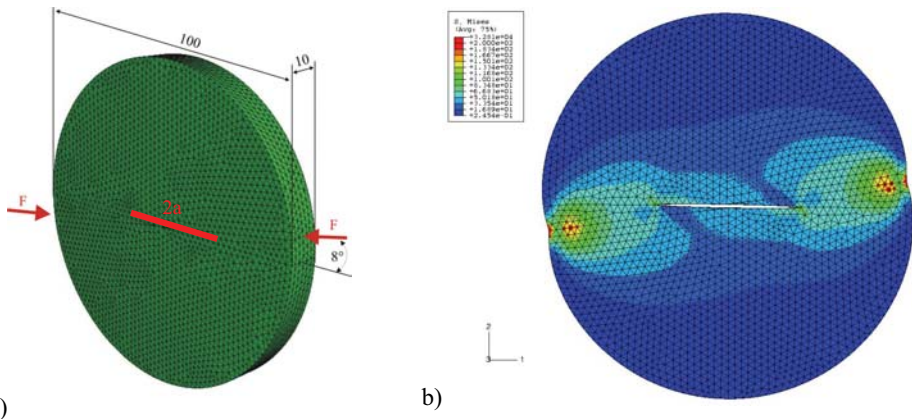


Figure 8: a) Brazilian disk specimen      b) Stress field for orthotropic material behaviour

The numerical example for orthotropic material behaviour is carried out for a Brazilian disk specimen as depicted in Figure 8. The specimen is loaded by two forces with a loading angle of  $8^\circ$  with respect to the crack axis. The crack length is set  $2a=40\text{mm}$  while the general boundary

conditions are chosen plain strain. The elastic material parameters for the orthotropic as well as for the isotropic reference case can be gathered from Table 1.

Table 1: Elastic Material parameters

	orthotropic material	isotropic material
$E_1$	10000 MPa	70656 MPa
$E_2$	8000 MPa	
$E_3$	6000 MPa	
$\nu_{12}$	0.1	0.34
$\nu_{23}$	0.3	
$\nu_{31}$	0.2	
$G_{12}$	4000 MPa	
$G_{13}$	6000 MPa	
$G_{23}$	5000 MPa	

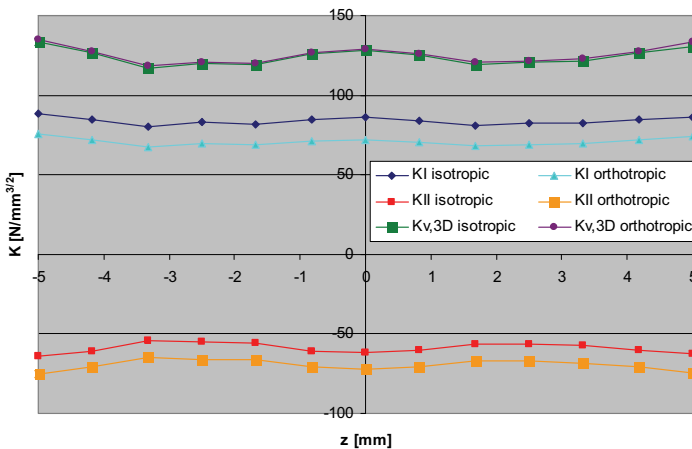


Figure 9: Stress intensity factor distribution for the Brazilian disc specimen for isotropic and orthotropic material behaviour

The results for both the isotropic and the orthotropic material are given in Figure 9. As consequence of the loading inclination angle of  $8^\circ$ , the crack fronts are subjected to a Mixed Mode loading situation with  $K_{I-}$  and  $K_{II-}$ portions of about the same magnitude ( $K_{I, iso}$   $85N/mm^{3/2}$ ,  $K_{II, iso}$   $60N/mm^{3/2}$  in the isotropic case). The distribution along the crack front is relatively even. It becomes apparent, that with respect to the reference isotropic solution (dark blue and red line) the Mode I-portion in the orthotropic case is a little smaller ( $K_{I, ortho}$   $70N/mm^{3/2}$ ), while at the same time the Mode II-portion notably increases ( $K_{II, ortho}$   $70N/mm^{3/2}$ ). Those value agree very well with findings by Banks-Sills et al. [7]. However, interestingly the equivalent stress intensity factors  $K_{v,3D}$  combining the contributions of the single Modes by means of the  $\sigma_1'$ -criterion[4], show a very good match for the isotropic and the orthotropic material.

## Conclusions

In this paper some extensions of the three-dimensional crack simulation program system ADAPCRACK3D are discussed. This program now is able to carry out crack propagation simulations for non-homogenous as well as non-isotropic material behaviour. Inhomogenous material is realized by the approach of a number of piecewise homogenous parts with interfaces. Therefore adjustments with respect to mesh generation were necessary. The calculation of stress intensities in orthotropic materials requires a different conversion from the originally calculated energy release rates. The given simulation examples yield good results with respect to known reference solutions and thus show the applicability of the extensions to industrial applications.

## Acknowledgement

This contribution is based on investigations of the collaborative research center SFB/TR TRR30, which is kindly supported by the DFG.

## References

- [1] M. Schöllmann, M. Fulland and H. A. Richard: Eng. Frac. Mech. 70 (2003), pp. 221-230.
- [2] F.G. Buchholz, in: *Accuracy, Reliability and Training in FEM Technology*, edited by J. Robinson, Robinson and Associates, Dorset (1984), pp. 650-659.
- [3] E.F. Rybicki and M.F. Kanninen: Eng. Frac. Mech. 9 (1977), pp. 931-938.
- [4] M. Schöllmann, G. Kullmer, M. Fulland and H.A. Richard, in: *Proc. of 6<sup>th</sup> Int. Conf. on Biaxial/Multiaxial Fatigue & Fracture*, edited by M. de Freitas (2001), Lisbon, pp. 589-596.
- [5] M. Fulland: *Rissimulationen in dreidimensionalen Strukturen mit automatischer adaptiver Finite-Elemente-Netzgenerierung* (Fortschritt-Bericht VDI, Reihe 18: Mechanik/Bruchmechanik Nr. 280, VDI-Verlag, Düsseldorf, 2003).
- [6] R. Pippin, K. Flechsig and F.O. Riemelmoser, in: *Materials Science and Engineering A283* (2000), pp. 225-233.
- [7] L. Banks-Sills, I. Hershkovitz, P.A. Wawrzynek, R. Eliasi and A.R. Ingraffea: Eng. Frac. Mech. 74 (2006), pp. 1293-1307.
- [8] G.C. Sih, P.C. Paris, G.R. Irwin, in: *Int. J. of Frac. Mech.* 1 (1965), pp. 189-203.